STEM CELLS®

REGENERATIVE MEDICINE

Genome Modification Leads to Phenotype Reversal in Human Myotonic Dystrophy Type 1 Induced Pluripotent Stem Cell-Derived Neural Stem Cells

GUANGBIN XIA,[a,b,c,d,e] YUANZHENG GAO,[a,d] SHOUGUANG JIN,[f] S.H. SUBRAMONY,[a,c,d] NAOHIRO TERADA,[b,g] LAURA P.W. RANUM,[a,c,f,h] MAURICE S. SWANSON,[c,f,h] TETSUO ASHIZAWA[a,b,c,d]

Key Words. Pluripotency • Neural Stem Cell • Gene targeting • Muscular dystrophy • Genomics • Cell transplantation

[a]Department of Neurology; [b]Center for Cellular Reprogramming; [c]Center for NeuroGenetics; [f]Department of Molecular Genetics and Microbiology; and [g]Department of Pathology, Immunology & Laboratory Medicine, College of Medicine, University of Florida, Gainesville, Florida, USA; [d]The Evelyn L & William F. McKnight Brain Institute; [e]Department of Neuroscience; and [h]Genetics Institute, University of Florida, Gainesville, Florida, USA

Correspondence: Guangbin Xia, M.D., Ph.D., Department of Neurology, Room L3–100, McKnight Brain Institute, 1149 S. Newell Drive, Gainesville, Florida 32611, USA. Telephone: 352-273-5550; Fax: 352-273-5575; e-mail: guangbin.xia@neurology.ufl.edu

Received November 1, 2014; accepted for publication January 17, 2015; first published online in STEM CELLS *EXPRESS* February 20, 2015.

1066-5099/2015/$30.00/0

http://dx.doi.org/10.1002/stem.1970

ABSTRACT

Myotonic dystrophy type 1 (DM1) is caused by expanded CTG repeats in the 3′-untranslated region (3′ UTR) of the *DMPK* gene. Correcting the mutation in DM1 stem cells would be an important step toward autologous stem cell therapy. The objective of this study is to demonstrate in vitro genome editing to prevent production of toxic mutant transcripts and reverse phenotypes in DM1 stem cells. Genome editing was performed in DM1 neural stem cells (NSCs) derived from human DM1 induced pluripotent stem (iPS) cells. An editing cassette containing SV40/bGH polyA signals was integrated upstream of the CTG repeats by TALEN-mediated homologous recombination (HR). The expression of mutant CUG repeats transcript was monitored by nuclear RNA foci, the molecular hallmarks of DM1, using RNA fluorescence in situ hybridization. Alternative splicing of microtubule-associated protein tau (*MAPT*) and muscleblind-like (*MBNL*) proteins were analyzed to further monitor the phenotype reversal after genome modification. The cassette was successfully inserted into *DMPK* intron 9 and this genomic modification led to complete disappearance of nuclear RNA foci. *MAPT* and *MBNL* 1, 2 aberrant splicing in DM1 NSCs were reversed to normal pattern in genome-modified NSCs. Genome modification by integration of exogenous polyA signals upstream of the *DMPK* CTG repeat expansion prevents the production of toxic RNA and leads to phenotype reversal in human DM1 iPS-cells derived stem cells. Our data provide proof-of-principle evidence that genome modification may be used to generate genetically modified progenitor cells as a first step toward autologous cell transfer therapy for DM1. STEM CELLS *2015;33:1829–1838*

INTRODUCTION

Myotonic dystrophy type 1 (DM1) is a dominantly inherited genetic disorder and the most common muscular dystrophy in adults. The disease is caused by an unstable CTG nucleotide expansion of >50 CTG repeats in the 3′-untranslated region (3′ UTR) of the *dystrophia myotonica* protein kinase (*DMPK*) gene on chromosome 19q13.3 [1]. The expanded repeat is transcribed into toxic CUG expansion RNAs, which sequester the MBNL family of splicing factors to form nuclear RNA foci. These RNA foci are the molecular hallmarks of DM1 and have been used as one of the outcome measures for DM1 therapeutic development. Muscleblind-like (*MBNL*) sequestration causes aberrant splicing of a large number of genes (see recent reviews) [2–6]. These aberrant splicing events have been proposed to contribute toward the multisystemic clinical presentation of DM1, including myotonia, diabetes, cardiac events, and cognitive impairment.

Multiple therapeutic approaches aimed at reducing mutant *DMPK* transcripts are being developed. These strategies, which include ribozymes, antisense oligonucleotides (ASOs/AONs) and small molecules, have shown promising results [7–13]. However, these approaches may be most effective at early stages of the disease because the mutant CUG transcript knockdown is not permanent, making these strategies challenging for long-term therapy. Cell replacement therapy could provide a viable alternative, especially for patients at an advanced disease stage.

Induced pluripotent stem (iPS) cells hold great promise for cell replacement therapy (see recent reviews) [14–17]. iPS cells can be derived from multiple somatic cells and can be differentiated into all three embryonic germ layer cells [18–22]. The capacity of iPS cells for

self-renewal provides a potential source for an unlimited number of cells. However, a major hurdle in the therapeutic application of iPS cells in genetic disorders is that patient-derived cells still carry the gene mutation so they may undergo a similar degenerative process after transplantation. For DM1, a dominant disease characterized by RNA gain-of-function [2, 5, 23–29], the ideal solution is targeted gene correction to prevent expression of expanded CTG repeats.

We have recently generated disease-specific DM1 iPS cell lines [30]. These DM1 iPS cell lines and their derivatives show pathogenic nuclear RNA foci. In this study, we tested the hypothesis that genome modification can be used to eliminate mutant transcripts and nuclear RNA foci in DM1 stem cells. Neural stem cells (NSCs) derived from DM1 iPS cells were chosen for this study because: (a) the CNS of patients with DM1 exhibits molecular, cellular, magnetic resonance imaging, and neuropsychological abnormalities [31–37]; (b) frontal executive dysfunction in adults and mental retardation in congenital and child-onset DM1 are some of the most disabling phenotypes of this multisystemic disease [38–45]; (c) technologies for cell transfer therapy in the central nervous system have shown promising recent advances (see recent reviews) [46–51]; (d) 100% of the NSCs are nuclear RNA foci positive and are amenable to single cell cloning so that the effect of gene correction can be tracked by monitoring nuclear RNA foci. Our approach was to introduce Simian virus 40 (SV40) and bovine growth hormone (bGH) polyA signals (PASs) upstream of the *DMPK* CTG expansion using homologous recombination (HR) mediated by a pair of site-specific transcription activator-like effector nucleases (TALEN). Both the SV40 and bGH PASs contain signals that promote 3′ end formation and polyadenylation [52, 53], which had been used previously to silence a noncoding RNA gene [54]. We have found that integration of these PASs upstream of the mutant CTG expansion prevented production of expanded CUG transcripts and led to the ablation of nuclear RNA foci and reversal of aberrant splicing.

Materials and Methods

Reagents

All restriction enzymes were from New England BioLabs (Ipswich, MA, https://www.neb.com). TALEN and targeting vectors were purified using the EndoFree Plasmid Maxi Kit (Qiagen, Valencia, CA, http://www1.qiagen.com). Cy3-labeled $(CAG)_{10}$ DNA probes were synthesized by Integrated DNA Technologies (Coralville, IA, https://www.idtdna.com).

TALEN Synthesis and Validation

The unique cutting site in *DMPK* intron 9 was identified by TAL Effector Nucleotide Targeter 2.0 (https://tale-nt.cac.cornell.edu/). TALEN binding sequence, Repeat-variable di-residues (RVDs), and the vector map (pTALEN) are listed in Supporting Information Figure 1A. TALENs were synthesized by Cellectis Bioresearch. (Cambridge, MA). TALEN validation was performed on HCT116 cells, and the activity was assessed by deep sequencing (Roche 454) of polymerase chain reaction (PCR) products from a pair of primers flanking the TALEN cutting site (forward primer: 5′-TGGCTCACACGTGTACTGA-3′; reverse primer: 5′-GGGGTATGAAGTGGCTGTCC-3′).

Donor Construction

The insertion cassette, which contained the selectable markers daGFP or the puromycin-resistance gene and the PASs, was assembled using standard cloning techniques. The 3-phosphoglycerate kinase (PGK) promoter and daGFP or puromycin-resistance gene were floxed so that they could be removed by Cre-recombinase leaving the PASs (560 bp) in the modified genome. Site-specific integration was mediated by incorporating homologous arms flanking the insertion cassette. Homologous arms (1.2 kb in each arm) were PCR amplified using high fidelity DNA polymerase (Platinum Pfx DNA Polymerase, Invitrogen, Carlsbad, CA, http://www.invitrogen.com). The homologous arms and the insertion cassette were assembled according to published methods [55] using a Multisite Gateway Three Fragment Vector Construction Kit (Invitrogen) to generate donor vectors, pDEST PGK-daGFP-SV40 poly A-bGH poly A (pDEST-daGFP) and pDEST PGK-puro-SV40 poly A-bGH poly A (pDEST-puro). The sequences of insertion cassettes are shown in Supporting Information Methods. The vector map (pDEST-puro) is shown in Supporting Information Figure 1B.

Cell Culture and Transfection

DM-03 NSCs were generated by neural induction of human DM-03 iPS cells [30]. These cells are nearly 100% foci-positive except for some cells at the end of cytokinesis (unpublished data). Cells were expanded and maintained in STEMdiff Neural Progenitor Medium (STEMCELL Technologies, Vancouver, BC, Canada, http://www.stemcell.com). Transfection was performed in six-well plates when cells (at P6) were 90% confluence using Lipofectamine LTX with Plus Reagent (Life Technologies/Invitrogen, Grand Island, NY, http://www.invitrogen.com) according to the manufacturer's protocol. Briefly, for each well, 1 μg of each pTALEN vector and 4 μg of targeting vector (pDEST-daGFP or pDEST-puro) were added to 300 μl Opti-MEM. Following addition of 6 μl Lipofectamine Plus, the sample was incubated for 5 minutes at room temperature (RT), followed by the addition of 15 μl Lipofectamine LTX and incubation for 30 minutes at RT. This mixture was added to each well containing 2 ml of STEMdiff Neural Progenitor Medium. The culture medium was changed to fresh medium after 8 hours and 48 hours later; confluent cells were either subjected to bulk sorting to select daGFP positive cells or screened for puromycin resistance.

Fluorescence Activated Cell Sorting and Puromycin Selection

Following transfection with pTALENs and donor pDEST-daGFP, the cells were fluorescence activated cell (FACS) sorted. Transfection efficiency varied between 2% and 8% (Supporting Information Fig. 2). To allow genome integration of the insertion cassette and RNA foci turnover, sorted cells were further cultured in a 24-well plate for 5 days prior to transfer to ibidi-Treat μ-slides (Ibidi GmbH, Martinsried, Germany) for RNA fluorescence in situ hybridization (RNA-FISH). DM-03 NSCs transfected with pTALENs and pDEST-puro were subjected to puromycin selection at a predetermined optimal concentration (0.4 μg/ml). Cells began dying 48 hours later, and resistant cells were growing in colonies on the 4th day after selection. Ten colonies were mechanically selected for RNA-

FISH and genotyping. For each colony, foci-positive cells were counted in three different fields, and 100 cells were counted in each field, and the percentage of foci positive cells averaged. For single cell cloning, puromycin-resistant and foci-negative NSCs from colonies 2 and 6 were subjected to single cell sorting on a 96-well plate. Five clones from each colony were propagated for further phenotype and genotype analysis.

Removal of Floxed Puromycin Selectable Marker by Cre Recombinase

Puromycin-resistant and foci-negative colonies were cultured in neural progenitor medium. Cells were treated at 70% confluence with Cre and green fluorescent protein (GFP) expressing adenovirus (Ad (RGD)-GFP-iCre, Vector Biolabs, Philadelphia, PA, http://www.vectorbiolabs.com/vbs/index.html) at a multiplicity of infection (MOI) of 10. In these prepackaged adenoviruses, the Cre recombinase and GFP are separated by the 2A peptide, which allows monitoring of infection efficiency, and 48 hours later the cells were observed for infection efficiency and harvested for RNA-FISH, DNA extraction, and PCR genotyping.

RNA-FISH

FISH was conducted as previously described [30]. Briefly, cells were plated onto ibidiTreat μ-slides, fixed in 10% buffered formalin phosphate and then dehydrated in prechilled 70% ethanol. The cells were hybridized with a Cy3-labeled $(CAG)_{10}$ DNA probe after pretreatment. After hybridization, the cells were washed three times in prewarmed 40% formamide/2$\times$ saline-sodium citrate (SCC) buffer for 30 minutes at 37°C and once in sterile PBS (pH 7.4) and mounted with Vectashield Mounting Medium with 4′,6-diamidino-2-phenylindole (DAPI) (Vector Laboratories, Burlingame, CA, http://www.vectorlabs.com). Images were obtained using an Olympus IX81-DSU Spinning Disk confocal microscope.

DNA/RNA Isolation, Genotyping PCR, Reverse Transcriptase PCR, and Triplet Repeat Primed PCR

Genomic DNA of individual colonies was isolated with the DNeasy Blood & Tissue Kit (Qiagen). Total RNA was isolated using TRI Reagent (Molecular Research Center, Cincinnati, OH) according to the manufacturer's protocol. Total RNA was treated with DNase I (Sigma, DNase I Amplification Grade), and 1 μg RNA was reverse transcribed in a total volume of 20 μl with SuperScript III First-Strand Synthesis System (Life Technologies) according to manufacturer's instructions. The level of genomic DNA contamination was assessed using paired samples with the same amount of RNA but omitting the reverse transcriptase. Primer sequences and PCR conditions can be found in Supporting Information Table 1. Triplet repeat primed PCR (TP-PCR) was performed according to a published protocol to conform cell DM1 status [56]. Briefly, TP-PCR assay was performed in 25 μl volume on 150 ng genomic DNA with primer combination of P5 5′-FAM-CTTCCCAGGCCTGCAG TTTGCCCATC-3′ 1 μM, P3R 5′-TAC GCA TCC CAG TTT GAG ACG-3′ (1 μM), P4CTG 5′-TAC GCA TCC GAG TTT GAG ACG TGC TGC TGC TGC TGC T-3′ (0.1 μM). PCR products were resolved by electrophoresis on an automatic sequencer. For PCR, reverse transcriptase PCR (RT-PCR), and TP-PCR, AmpliTaq Gold 360 Master Mix (Life Technologies) was used.

MAPT and *MBNL* 1, 2 Alternative Splicing Assay

Normal NSC, DM-03 NSC, clone 2-3, clone 6-4 cells were cultured in six-well plates until 90% confluence. Cells were collected, and RNA was extracted for cDNA synthesis as described above. RT-PCR of *MAPT* gene spanning exon 2, 3, 4 was performed with primers: Tau F 5′-TACGGGTTGGGGG ACAGGAAACAT-3′ and Tau R 5′-GGGGTGTCTCCAATGCC TGCTTCT-3′ at condition of 94°C for 5 minutes, followed by 37 cycles of 94°C 30 seconds, 65°C 1 minute, and 72°C 1 minute as described before [57]. RT-PCR of *MBNL* 1 and 2 gene spanning exon 7 was performed with primers: MBNL1F 5′-GCTGCCCAATACCAGGTCAAC-3′ and MBNL1R 5′-TGGTGGG AGAAATGCTGTATGC-3′ for *MBNL* 1; MBNL2F 5′-ACAAGTGACA ACACCGTAACCG-3′ and MBNL2R 5′-TTTGGTAAAGGA TGAAGAGCACC-3′ for *MBNL* 2 at condition of 94°C for 5 minutes, followed by 37 cycles of 94°C 30 seconds, 58°C 30 seconds, and 72°C 1 minute as described before [58]. The intensity of each band on electrophoresis gel images was analyzed by Alphaview. The percentage of exon 2 inclusion in *MAPT* and exon 7 exclusin in *MBNL* 1, 2 was calculated (three independent experiments). Student's *t* test was used for statistics, and $p < .05$ was accepted as statistically significant.

Results

Overview of Targeting Strategy and TALEN Activity

As illustrated in Figure 1A, we introduced the SV40 and bGH PASs into *DMPK* intron 9 using a pair of TALENs. Intron 9 was chosen to allow the use of a long 3′ HR arm that does not span the *DMPK* CTG repeats. TALENs generate a double-strand break, which can be repaired by HR that allows integration of the insertion cassette containing the selectable markers (daGFP or the puromycin-resistance gene) and the PASs and thus block production of expanded CUG repeats. We expected the CUG repeat RNA foci would disappear in green fluorescent cells or puromycin-resistant cells that have integrated the cassette into the mutant *DMPK* allele. The selectable markers were flanked by two LoxP sites so that they could be removed by transient expression of Cre recombinase. TALENs caused mutagenesis (Indels) at the rate of 40% (total number of analyzed sequences: 3,744; number of WT sequences: 2,248; number of mutated sequences: 1,496 of which insertions = 11.1%, deletions = 87.7%, Indels = 1.2%). The most frequent Indels are listed in Figure 1B. The most frequent insertion was between 3 and 6 bp and the longest was 239 bp. Of the 12 long insertions (>100 bp), 9 were from different parts of the TALEN vector and 3 were from the human genome.

Absence of Nuclear RNA Foci in DM1 NSCs Transfected with TALEN and Donor Vectors

The majority of parental DM-03 NSCs contained nuclear RNA foci except for some cells, possibly in late telophase of mitosis that have cytoplasmic foci instead of intranuclear foci (Fig. 2A). We expected that nuclear RNA foci would not be present in GFP positive cells that had integrated the cassette into the mutant *DMPK* allele. After sorting DM-03 NSCs transfected with the pTALENs and pDEST-daGFP, we found approximately 15% of the sorted GFP positive cells showed no nuclear RNA

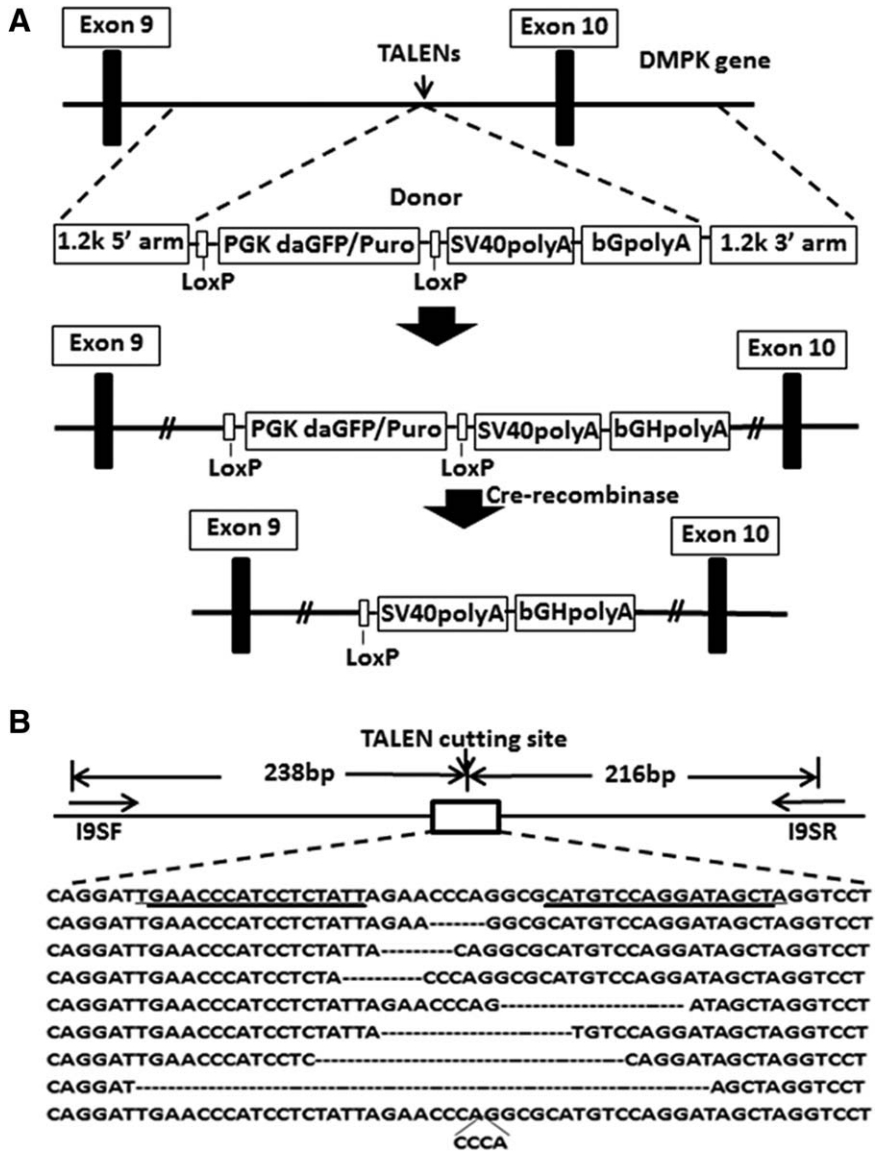

Figure 1. Schematic overview of targeting strategy and TALEN activity. **(A):** Insertion cassette containing PGK-daGFP (or puro)-SV40polyA-bGHpolyA flanked by 1.2 kb homologous arms targeting *DMPK* intron 9. A pair of site-specific TALENs creates a double stranded break (DSB) that is repaired by homologous recombination with the donor-containing insertion cassette. Selectable makers may be removed by transient expression of Cre recombinase, leaving only 560 bp, including the polyA signals, in the genome. **(B):** Normal sequence (top) and underlined sequences are the left and right TALEN recognition sites. DSBs induced by TALENs are repaired with insertions or deletions with the most frequent deletions listed below the normal sequence). The most frequent insertions are from 3 to 6 bp (single example shown). Abbreviations: DMPK, *dystrophia myotonica* protein kinase; PGK, 3-phosphoglycerate kinase; TALEN, transcription activator-like effector nucleases.

foci (Fig. 2B), indicating that these cells had the cassette integrated into the mutant *DMPK* allele. In the remaining daGFP negative cells (85%), intranuclear foci remained suggesting that either the wild-type allele was targeted or a random insertion event had occurred or from remaining transient expression of the plasmid (Fig. 2C). Since the GFP signal in the merged images affect the visualization of foci, images with and without GFP channel were arranged in parallel to better visualize the foci (Supporting Information Fig. 3).

In cells that were transfected with the pTALENs and pDEST-puro, colonies started forming after 7 days of selection with puromycin. Of 10 selected colonies, 4 showed no nuclear RNA foci in the majority of cells (Fig. 2D, 2E), 3 colonies showed a majority of cells containing intranuclear foci (Fig. 2F, 2G) and the remaining 3 had a mixed population of cells with/without nuclear RNA foci (not shown). The percentage of foci-positive cells was counted in each group. Colonies 2 and 6 which were later used for single cell cloning showed significantly fewer cells positive for nuclear RNA foci than parental cells and colonies 1 and 7 (Fig. 2H). The disappearance of nuclear RNA foci suggests that mutant CUG repeat expression was prevented by integration of the exogenous PASs upstream of the CTG repeat expansion in the mutant allele. The persistence of nuclear RNA foci in some of the puromycin-resistant colonies was likely due to integration into the wild-type *DMPK* allele or a random insertion event.

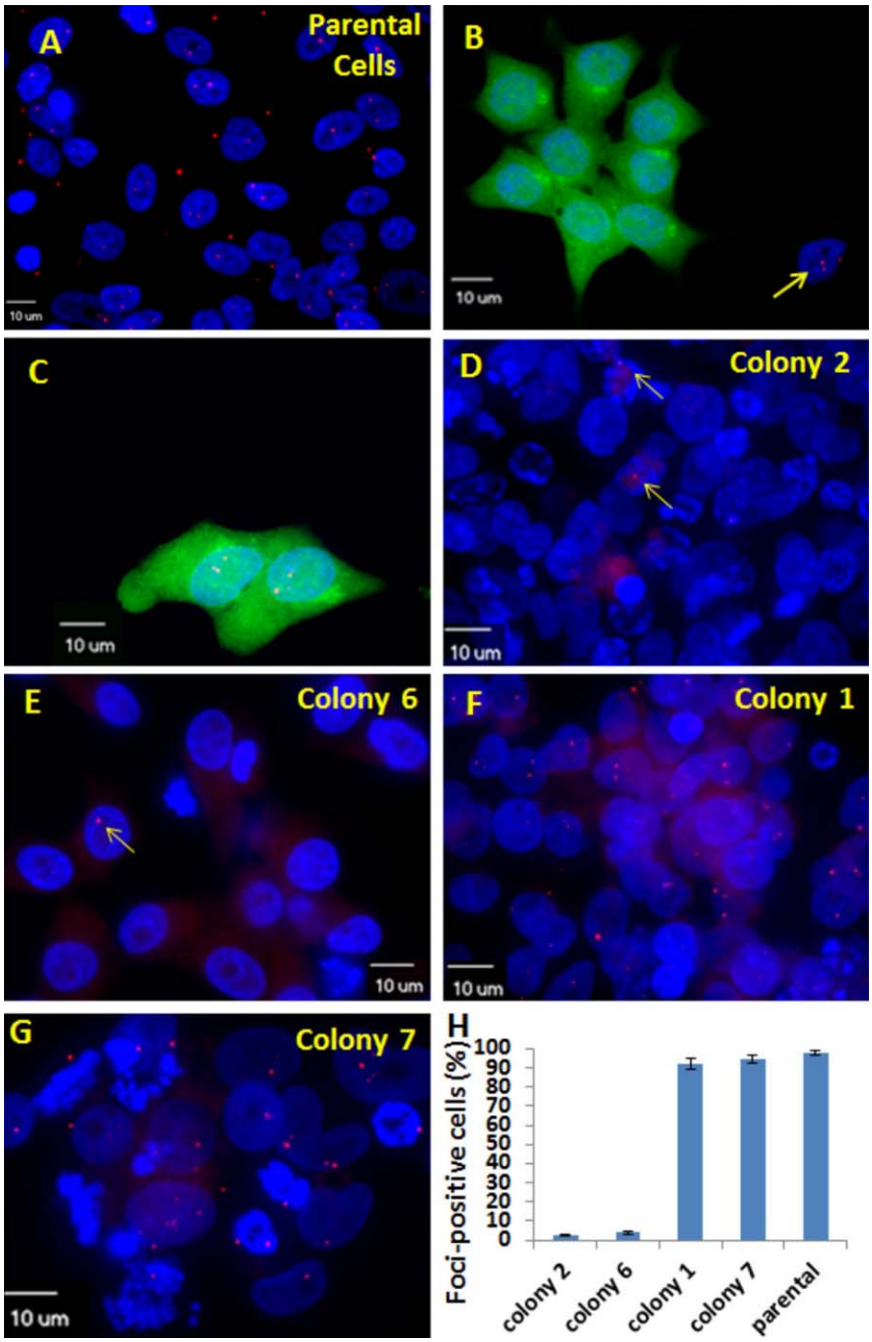

Figure 2. Loss of nuclear RNA foci in Myotonic dystrophy type 1 (DM1) neural stem cells (NSCs) transfected with pTALENs and donor vectors. **(A):** Parental DM-03 NSCs with prevalent nuclear RNA foci. Cytoplasmic foci were also frequently present in proliferating cells. **(B):** Nuclear RNA foci were not detectable in a subset of daGFP positive cells, suggesting the cassette was inserted in the mutant allele, while in daGFP negative cells, RNA foci were routinely observed as internal control of fluorescence in situ hybridization (arrow). **(C):** Nuclear RNA foci remained in a subset of daGFP positive cells, suggesting integration into normal allele or random insertion. **(D, E):** In some puromycin-resistant colonies of DM-03 NSC, nuclear RNA foci were absent in the majority of cells although occasional foci were detectable (arrows). **(F, G):** Nuclear RNA foci were detectable in the majority of Colony 1 and 7 cells. **(H):** The percentage of foci-positive cells in selected colonies and parental cells. The error bars are SD of the percentage of foci-positive cells in three isolated areas in the same slide.

Analysis of Exogenous TALEN-Mediated PAS Integration

Puromycin-resistant colonies might result from integration of the insertion cassette into either the normal or mutant allele or both. Insertion into the mutant allele would lead to disappearance of intranuclear foci while integration into the wild-type allele alone should not affect RNA foci formation. If the insertion cassette integrated into both the mutant and wild-type alleles, foci should be abolished with no production of the full-length *DMPK* mRNA. To confirm that the lack of RNA foci in cells transfected with pTALENs and pDEST-puro was the

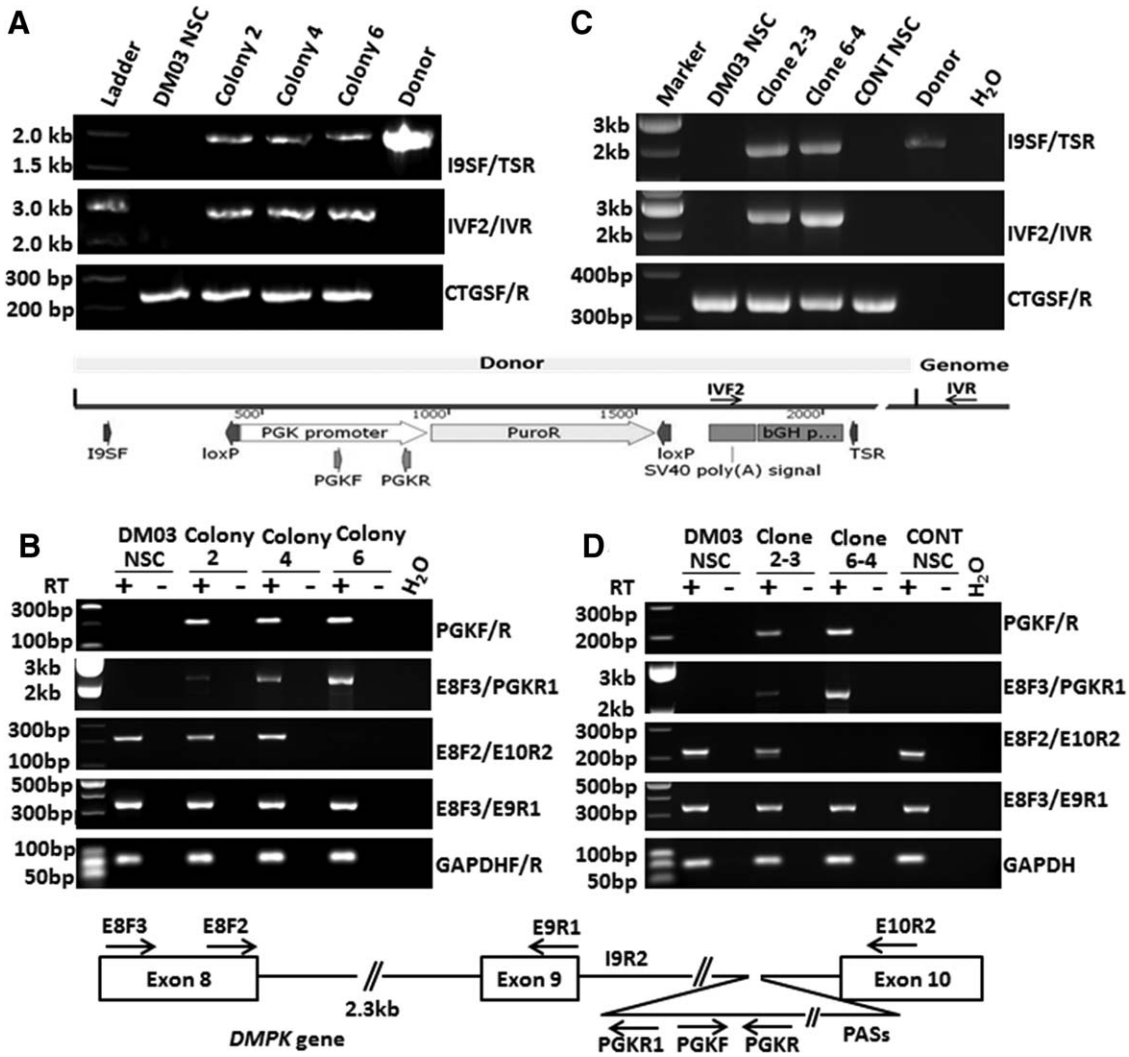

Figure 3. Exogenous PASs were integrated in the transcription activator-like effector nucleases (TALEN) targeting site and was transcribed contiguous with *DMPK* transcription. **(A):** Polymerase chain reaction (PCR) analysis showing the integration of insertion cassette into the TALEN targeting site. Primer pair I9SF/TSR amplified the whole insertion cassette, detectable in puromycin-resistant clones and donor vector but not in parental cells (upper panel). Primer pair IVF2/IVR amplified a portion of the insertion cassette and a portion of genomic DNA downstream of the end of the 3′ homology arm (middle panel). CTGSF/CRGSR amplified genomic DNA as a template loading control. **(B):** Reverse transcriptase PCR (RT-PCR) showing the effect of the integration on DMPK gene transcription. Products from primer pair PGKF/PGKR and E8F3/PGKR1 were detected in the three puromycin-resistant, foci-negative colonies but not in the parental cells. Products from E8F2/E10R2, which spans exon 8, 9, 10 and long introns, indicated normal DMPK transcription in parental cells and colonies 2, 4 from the unaffected allele and the lack of a product in colony 6 suggests both alleles were targeted. Products from E8F3/E9R1 suggested upstream mRNA was intact in all of the colonies. GAPDH was amplified as a reverse transcription control. **(C, D):** PCR and RT-PCR analyses of single cell clones. The integration of the insertion cassette and the same effect on DMPK gene transcription were confirmed in single cell clones. +: with reverse transcriptase. −: No reverse transcriptase. Clone 2–3 was from colony 2. Clone 6-4 was from colony 6. Abbreviations: CONT NSC: normal NSC derived from normal iPS cells; DMPK, *dystrophia myotonica* protein kinase; PASs, polyA signals; PGK, 3-phosphoglycerate kinase; NSC, neural stem cell.

result of the introduction of the PASs into the TALEN cutting site, PCR genotyping was performed. Detection of the PCR product from primer pair I9SF/TSR, which flanked the whole insertion cassette and was also part of 5′ homologous arm, indicated integration of the insertion cassette into the genome (Fig. 3A, top panel) although not necessarily at the TALEN cutting site. To verify that insertion occurred at the designed TALEN cutting site (intron 9), a primer pair (IVF2/IVR) was designed to flank part of the insertion cassette and 862 bp downstream of the 3′ homology arm. These primers generated the anticipated PCR product (Fig. 3A, middle panel), which was confirmed by DNA sequencing, thus demonstrating that the insertion cassette was introduced into intron 9. To verify that the insertion cassette was transcribed contiguous with *DMPK* transcription, we performed RT-PCR analysis to amplify the PGK promoter (PGKF/PGKR) of the insertion cassette and a portion of intron 9 (E8F3/PGKR1) in puromycin-resistant and foci-negative colonies. As shown in Figure 3B, the anticipated products were correctly amplified by RT-PCR. The primer pair of E8F3/PGKR1 spans a portion of exon 8, intron 8, exon 9, intron 9 before the insertion site and a portion of PGK promoter. After sequencing the product,

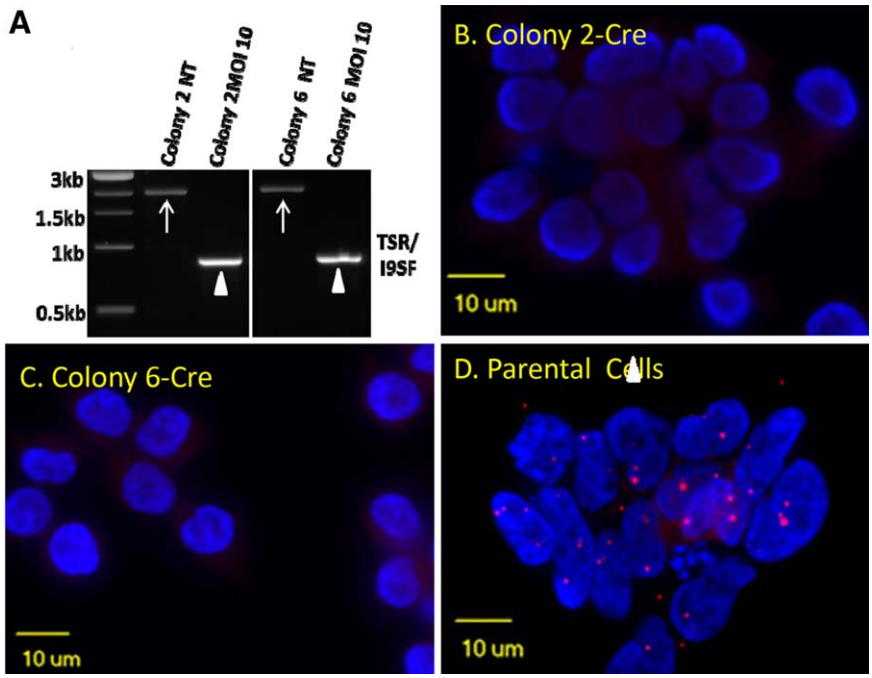

Figure 4. Targeted cells remained RNA foci-negative after removal of the puromycin selectable marker. **(A):** Following infection with Ad (RGD)-GFP-iCre, floxed puromycin resistant gene cassettes were removed in both colonies 2 and 6. The size of the polymerase chain reaction products flanked by I9SF/TSR decreased from 2,014 bp (arrows) in noninfected cells to 860 bp (arrowheads) in infected cells. Colony 2-Cre **(B)** and colony 6-Cre **(C)** continued to be RNA foci free after removal of the selectable markers but retention of the exogenous PASs while the parental cells **(D)** were foci-positive.

we found that intron 8 was spliced out while intron 9 was retained and extended to the PGK promoter toward PASs (Supporting Information Fig. 4). In colonies 2 and 4, wild-type *DMPK* transcription was preserved, which was confirmed by primers (E8F2/E10R2) that flanks exons 8, 9, and 10, suggesting that the wild-type allele in these puromycin-resistant colonies was not targeted. For colony 6, the E8F2/E10R2 primers failed to amplify a product suggesting both alleles were targeted. The existence of an RT-PCR product from E8F3/E9R1 suggests upstream mRNA was intact in all the colonies, including colony 6. Single cell cloning was also conducted and five clones, which were generated from colonies 2 and 6, were all foci-negative (Supporting Information Fig. 5) and PCR genotyping again showed the same PAS integration into intron 9 and the effect on *DMPK* transcription (Fig. 3C, 3D).

Cells Remained RNA Foci-Negative After Removal of the Selectable Marker

To confirm that introduction of the exogenous PASs alone was sufficient to prevent the production of RNA foci, the floxed PGK-puromycin portion of the integrated cassette was removed by transient expression of Cre recombinase using Ad (RGD)-GFP-iCre. The infection efficiency of Ad(RGD)-GFP-iCre reached nearly 100% at an MOI = 10 (Supporting Information Fig. 6). PCR genotyping showed successful removal of the puromycin selectable marker (Fig. 4A), and the cells continued to be foci-free (Fig. 4B, 4C) while parental cells were all foci-positive (Fig. 4D). TP-PCR confirmed the presence of the CTG repeat in these cells with a typical saw-tooth pattern by capillary electrophoresis with CTG repeat $>$ 136 (the limit of this test discrimination) (Supporting Information Fig. 7).

MAPT and *MBNL* 1, 2 Aberrant Splicing have been Reversed in Genome-Modified Clones

To reinforce the proof of concept of ablation of RNA nuclear foci, we further evaluate the splicing pattern of *MAPT*, which has been shown to have decreased inclusion of exon 2, and *MNBL* 1, 2, which have been shown to have deceased exclusion of exon 7 in CNS in DM1. We found the splicing patterns have been reversed to normal patterns as in normal NSC (Fig. 5).

Discussion

Genome modification has been widely used for gene targeting to study gene functions [59–66]. More recently, this strategy has been exploited to correct point mutations in some monogenic human disease-specific cells, including iPS cells for therapeutic development [67–70]. However, correction of repeat expansion mutations in the unstable microsatellite diseases, including DM1, DM2, repeat expansion-mediated SCAs, HD, and *C9ORF72* ALS/FTD, remains a challenge. Multiple therapeutic approaches are possible, including targeted deletion of the entire tandem repeat region or targeted shortening of the expansion. For targeted deletion, two simultaneous double-strand breaks (DSB) flanking the tandem repeat region must be created, which is technically more challenging since repeats in DM1 somatic cells may be $>$1,000. For targeted repeat deletions, the repeat itself will be the target but a major concern is off-target effects since many genes contain CTG repeats. In this study, we have tested the approach of introducing PASs upstream of the CTG expansion to prevent production of expanded CUG repeats. Introduction of

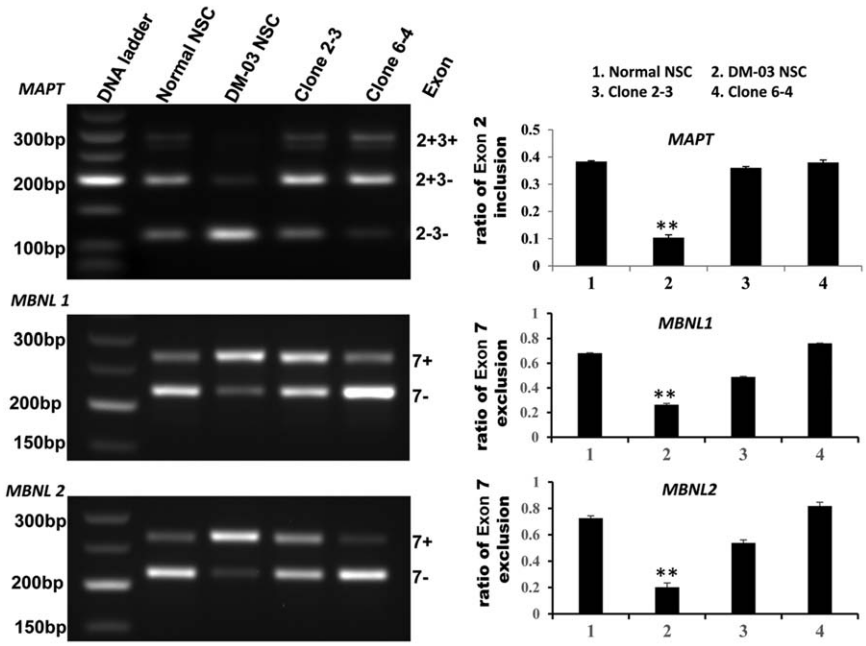

Figure 5. Genome modification reversed aberrant splicing of *MAPT* and *MBNL* 1, 2 in DM1 to normal pattern. Exon 2 inclusion of *MAPT* is significantly decreased in DM1–03 NSCs compared to normal NSCs (**, $p < .01$) but the pattern was completely reversed in the genome-modified clone 2–3 and 6-4 (upper panel). The ratio of exon 7 exclusion of *MBNL* 1, 2 was significantly decreased in DM-03 NSCs compared to normal NSCs (**, $p < .01$)) but the patterns were reversed in genome-modified clone 2–3 and 6-4 (middle and lower panels). Abbreviations: *MAPT*, microtubule associated protein tau; *MBNL*, muscleblind-like protein; NSC, neural stem cell.

exogenous PASs into the mutant *DMPK* intron 9 ablated RNA foci, the toxic transcripts in DM1, which was reinforced by the reversal of aberrant splicing of *MAPT* and *MBNL* 1, 2 genes that have been shown in DM1 CNS [37, 57, 58]. Insertion of these PASs should trigger 3′ end cleavage and polyadenylation in intron 9 [52, 53], and the resulting downstream transcripts should be degraded even if they reached expanded repeats. When no donor DNA exists, the DSB will be annealed by nonhomologous end joining (NHEJ), which is an error-prone repair mechanism [66]. Even with the existence of donors, NHEJ still competes with HR, a common observation in human cells [71]. Since the coding sequence should be avoided for TALEN targeting using the PAS strategy, we selected intron 9 as the integration site, which is predicted to generate a truncated DMPK protein since a stop codon is introduced immediately after exon 9. Interestingly, this truncated protein may exist naturally due to alternative DMPK pre-mRNA splicing and intron 9 retention occurs in both DM1 and non-DM1 NSCs and fibroblasts (Supporting Information Fig. 8). The truncated protein misses the C-terminal which is important for localization but contains the whole catalytic kinase domains including downstream VSGGG motif which has been shown to be a key element for DMPK autophosphorylation and phosphorylation of its targets [72]. Whether this truncated protein will still be functional or create dominant-negative effects, however, is unknown. In clone 6-4, only truncated protein is predicted to be expressed. This clone will serve well for studying the functions of this truncated protein. Nevertheless, the ideal insertion site is between the normal *DMPK* stop codon and the 5′ end of CTG repeat expansion since this approach might maintain normal expression of the wild-type *DMPK* protein even if both alleles are targeted. This latter approach was not pursued in this study because only 234 bp exist between the *DMPK* stop codon and the CTG repeat region and thus it was problematic to design a long 3′ HR arm. Currently, we are attempting to use the expanded CTG repeat region as a unique arm for specific mutant allele targeting between the normal stop codon and the 5′ end of the CTG repeat expansion region.

The experimental approach used in this study does not differentiate normal from mutant alleles. Selection of single clones is required to obtain clones in which only the mutant allele is modified while the wild type allele is unaffected so deleterious effects on *DMPK* protein levels are minimized. In this study, the general transfection efficiency was <8%, and the efficiency of biallelic targeting was considerably lower. Indeed, out of 10 colonies, we identified only one colony in which both alleles had been targeted. Although this study was conducted using NSCs, the same targeting approach can be applied to iPS cells. The growth pattern and the trait of infinite self-renewal of iPS cells will facilitate clone selection. Moreover, iPS cells can be differentiated into all three embryonic germ layer cells, which should have broader clinical application for cell-based therapies. The pathogenesis of noncoding microsatellite expansion disorders has unveiled some new functions for tandem repeat expansions, including repeat associated non-ATG (RAN) translation [73, 74]. Since there is increasing evidence that RAN translation plays an important role in the pathogenesis of these disorders, an advantage of the experimental approach described here is that elimination of the expanded CUG repeat will eliminate the possibility of RAN translation from the *DMPK* sense strand [73, 75–78].

Conclusion

In conclusion, we have demonstrated that genome modification by integration of exogenous PASs upstream of the *DMPK* CTG repeat expansion can prevent the production of toxic mutant transcripts and leads to phenotype reversal in human DM1 iPS-cells derived stem cells. Our data provide proof-of-principle evidence that genome modification may be used to generate genetically modified stem cells as a first step toward autologous cell transfer therapy for DM1. The same approach can be applied to other dominantly inherited gain-of-function microsatellite expansion disorders.

Acknowledgment

Research reported in this publication was supported by NIH/NIAMS grant K08 AR064836-01 to G.X.

Author Contributions

G.X., T.A., M.S.S., L.P.W.R., N.T., and S.J.: study conception and design; G.X. and Y.G.: data acquisition; G.X, T.A., M.S.S., L.P.W.R., N.T., S.J., and Y.G: analysis and interpretation; G.X., T.A., M.S.S., T.R., N.T., S.J., and S.H.S.: manuscript preparation.

Disclosure of Potential Conflicts of Interest

Dr. Subramony has received an honorarium to speak on genetic disorders of cerebellum from Athena Diagnostics. Dr. Ranum has a patent Gene sequence for spinocerebellar ataxia type 1 and methods for diagnosis (Patent #5,834,183), November 10, 1998, with royalties paid; a patent SCA7 Gene and Method of Use (Patent # 6,280,938) with royalties paid; a patent Spinocerebellar ataxia type 8 and methods of detection (Patent # 6,524,791) issued; a patent Identification of a gene associated with spinocerebellar ataxia type 5 and methods of use (patent # 7527931) issued; a patent Repeat associated non-ATG translation and Methods of Use pending; and a patent Use and treatment of repeat associated non-ATG proteins associated with ALS pending. The other authors indicate no potential conflicts of interest.

References

1 Fu YH, Pizzuti A, Fenwick RG, Jr. et al. An unstable triplet repeat in a gene related to myotonic muscular dystrophy. Science 1992;255:1256–1258.

2 Ashizawa T, Sarkar PS. Myotonic dystrophy types 1 and 2. Handb Clin Neurol 2011;101:193–237.

3 Romeo V. Myotonic Dystrophy Type 1 or Steinert's disease. Adv Exp Med Biol 2012;724:239–257.

4 Ranum LP, Cooper TA. RNA-mediated neuromuscular disorders. Annu Rev Neurosci 2006;29:259–277.

5 Lee JE, Cooper TA. Pathogenic mechanisms of myotonic dystrophy. Biochem Soc Trans 2009;37:1281–1286.

6 Gomes-Pereira M, Cooper TA, Gourdon G. Myotonic dystrophy mouse models: Towards rational therapy development. Trends Mol Med 2011;17:506–517.

7 Wheeler TM, Sobczak K, Lueck JD et al. Reversal of RNA dominance by displacement of protein sequestered on triplet repeat RNA. Science 2009;325:336–339.

8 Lee JE, Bennett CF, Cooper TA. RNase H-mediated degradation of toxic RNA in myotonic dystrophy type 1. Proc Natl Acad Sci USA 2012;109:4221–4226.

9 Langlois MA, Lee NS, Rossi JJ et al. Hammerhead ribozyme-mediated destruction of nuclear foci in myotonic dystrophy myoblasts. Mol Ther 2003;7:670–680.

10 Warf MB, Nakamori M, Matthys CM et al. Pentamidine reverses the splicing defects associated with myotonic dystrophy. Proc Natl Acad Sci USA 2009;106:18551–18556.

11 Mulders SA, van den Broek WJ, Wheeler TM et al. Triplet-repeat oligonucleotide-mediated reversal of RNA toxicity in myotonic dystrophy. Proc Natl Acad Sci USA 2009;106:13915–13920.

12 Wheeler TM, Leger AJ, Pandey SK et al. Targeting nuclear RNA for in vivo correction of myotonic dystrophy. Nature 2012;488:111–115.

13 Parkesh R, Childs-Disney JL, Nakamori M et al. Design of a bioactive small molecule that targets the myotonic dystrophy type 1 RNA via an RNA motif-ligand database and chemical similarity searching. J Am Chem Soc 2012;134:4731–4742.

14 Drews K, Jozefczuk J, Prigione A et al. Human induced pluripotent stem cells—From mechanisms to clinical applications. J Mol Med (Berl) 2012;90:735–745.

15 Ebben JD, Zorniak M, Clark PA et al. Introduction to induced pluripotent stem cells: Advancing the potential for personalized medicine. World Neurosurg 2011;76:270–275.

16 Lengner CJ. iPS cell technology in regenerative medicine. Ann N Y Acad Sci 2010;1192:38–44.

17 Wu SM, Hochedlinger K. Harnessing the potential of induced pluripotent stem cells for regenerative medicine. Nat Cell Biol 2011;13:497–505.

18 Takahashi K, Tanabe K, Ohnuki M et al. Induction of pluripotent stem cells from adult human fibroblasts by defined factors. Cell 2007;131:861–872.

19 Aasen T, Raya A, Barrero MJ et al. Efficient and rapid generation of induced pluripotent stem cells from human keratinocytes. Nat Biotechnol 2008;26:1276–1284.

20 Meissner A, Wernig M, Jaenisch R. Direct reprogramming of genetically unmodified fibroblasts into pluripotent stem cells. Nat Biotechnol 2007;25:1177–1181.

21 Sun N, Panetta NJ, Gupta DM et al. Feeder-free derivation of induced pluripotent stem cells from adult human adipose stem cells. Proc Natl Acad Sci USA 2009;106:15720–15725.

22 Boulting GL, Kiskinis E, Croft GF et al. A functionally characterized test set of human induced pluripotent stem cells. Nat Biotechnol 2011;29:279–286.

23 Mankodi A, Logigian E, Callahan L et al. Myotonic dystrophy in transgenic mice expressing an expanded CUG repeat. Science 2000;289:1769–1773.

24 Seznec H, Agbulut O, Sergeant N et al. Mice transgenic for the human myotonic dystrophy region with expanded CTG repeats display muscular and brain abnormalities. Hum Mol Genet 2001;10:2717–2726.

25 Orengo JP, Chambon P, Metzger D et al. Expanded CTG repeats within the DMPK 3' UTR causes severe skeletal muscle wasting in an inducible mouse model for myotonic dystrophy. Proc Natl Acad Sci USA 2008;105:2646–2651.

26 O'Rourke JR, Swanson MS. Mechanisms of RNA-mediated disease. J Biol Chem 2009;284:7419–7423.

27 Klein AF, Gasnier E, Furling D. Gain of RNA function in pathological cases: Focus on myotonic dystrophy. Biochimie 2011;93:2006–2012.

28 Todd PK, Paulson HL. RNA-mediated neurodegeneration in repeat expansion disorders. Ann Neurol 2010;67:291–300.

29 Dick KA, Margolis JM, Day JW et al. Dominant non-coding repeat expansions in human disease. Genome Dyn 2006;1:67–83.

30 Xia G, Santostefano KE, Goodwin M et al. Generation of neural cells from DM1 induced pluripotent stem cells as cellular model for the study of central nervous system neuropathogenesis. Cell Reprogram 2013;15:166–177.

31 Romeo V, Pegoraro E, Ferrati C et al. Brain involvement in myotonic dystrophies: Neuroimaging and neuropsychological comparative study in DM1 and DM2. J Neurol 2010;257:1246–1255.

32 Ogata A, Terae S, Fujita M et al. Anterior temporal white matter lesions in myotonic dystrophy with intellectual impairment: An

MRI and neuropathological study. Neuroradiology 1998;40:411–415.
33 Maurage CA, Udd B, Ruchoux MM et al. Similar brain tau pathology in DM2/PROMM and DM1/Steinert disease. Neurology 2005; 65:1636–1638.
34 Yoshimura N, Otake M, Igarashi K et al. Topography of Alzheimer's neurofibrillary change distribution in myotonic dystrophy. Clin Neuropathol 1990;9:234–239.
35 Mitake S, Inagaki T, Niimi T et al. [Development of Alzheimer neurofibrillary changes in two autopsy cases of myotonic dystrophy]. Rinsho Shinkeigaku 1989;29:488–492.
36 Kiuchi A, Otsuka N, Namba Y et al. Presenile appearance of abundant Alzheimer's neurofibrillary tangles without senile plaques in the brain in myotonic dystrophy. Acta Neuropathol 1991;82:1–5.
37 Jiang H, Mankodi A, Swanson MS et al. Myotonic dystrophy type 1 is associated with nuclear foci of mutant RNA, sequestration of muscleblind proteins and deregulated alternative splicing in neurons. Hum Mol Genet 2004;13:3079–3088.
38 Sistiaga A, Urreta I, Jodar M et al. Cognitive/personality pattern and triplet expansion size in adult myotonic dystrophy type 1 (DM1): CTG repeats, cognition and personality in DM1. Psychol Med 2010;40:487–495.
39 Bird TD, Follett C, Griep E. Cognitive and personality function in myotonic muscular dystrophy. J Neurol Neurosurg Psychiatry 1983;46:971–980.
40 Portwood MM, Wicks JJ, Lieberman JS et al. Intellectual and cognitive function in adults with myotonic muscular dystrophy. Arch Phys Med Rehabil 1986;67:299–303.
41 Roig M, Balliu PR, Navarro C et al. Presentation, clinical course, and outcome of the congenital form of myotonic dystrophy. Pediatr Neurol 1994;11:208–213.
42 Rubinsztein JS, Rubinsztein DC, McKenna PJ et al. Mild myotonic dystrophy is associated with memory impairment in the context of normal general intelligence. J Med Genet 1997;34:229–233.
43 Steyaert J, Umans S, Willekens D et al. A study of the cognitive and psychological profile in 16 children with congenital or juvenile myotonic dystrophy. Clin Genet 1997;52:135–141.
44 Ekstrom AB, Hakenas-Plate L, Samuelsson L et al. Autism spectrum conditions in myotonic dystrophy type 1: a study on 57 individuals with congenital and childhood forms. Am J Med Genet B Neuropsychiatr Genet 2008;147B:918–926.
45 Douniol M, Jacquette A, Guile JM et al. Psychiatric and cognitive phenotype in children and adolescents with myotonic dystrophy. Eur Child Adolesc Psychiatry 2009;18: 705–715.
46 Liu S, Li C, Xing Y et al. Effect of transplantation of human embryonic stem cell-derived neural progenitor cells on adult neurogenesis in aged hippocampus. Am J Stem Cells 2014;3:21–26.
47 Chen L, Qiu R, Xu Q. Mesenchymal stem cell therapy for neurodegenerative diseases. J Nanosci Nanotechnol 2014;14:969–975.
48 de Munter JP, Melamed E, Wolters E. Stem cell grafting in parkinsonism—Why, how and when. Parkinsonism Relat Disord 2014;20(suppl 1):S150–S153.
49 Thomsen GM, Gowing G, Svendsen S et al. The past, present and future of stem cell clinical trials for ALS. Exp Neurol 2014; 262:127–137.
50 Choi SS, Lee SR, Kim SU et al. Alzheimer's disease and stem cell therapy. Exp Neurobiol 2014;23:45–52.
51 Im W, Kim M. Cell therapy strategies vs. paracrine effect in Huntington's disease. J Mov Disord 2014;7:1–6.
52 Davila Lopez M, Samuelsson T. Early evolution of histone mRNA 3' end processing. RNA 2008;14:1–10.
53 Liu D, Brockman JM, Dass B et al. Systematic variation in mRNA 3'-processing signals during mouse spermatogenesis. Nucleic Acids Res 2007;35:234–246.
54 Gutschner T, Baas M, Diederichs S. Noncoding RNA gene silencing through genomic integration of RNA destabilizing elements using zinc finger nucleases. Genome Res 2011;21:1944–1954.
55 Iiizumi S, Nomura Y, So S et al. Simple one-week method to construct gene-targeting vectors: application to production of human knockout cell lines. Biotechniques 2006;41:311–316.
56 Warner JP, Barron LH, Goudie D et al. A general method for the detection of large CAG repeat expansions by fluorescent PCR. J Med Genet 1996;33:1022–1026.
57 Dhaenens CM, Tran H, Frandemiche ML et al. Mis-splicing of Tau exon 10 in myotonic dystrophy type 1 is reproduced by overexpression of CELF2 but not by MBNL1 silencing. Biochim Biophys Acta 2011;1812:732–742.
58 Hernandez-Hernandez O, Sicot G, Dinca DM et al. Synaptic protein dysregulation in myotonic dystrophy type 1: Disease neuropathogenesis beyond missplicing. Rare Dis 2013;1:e25553.
59 Li T, Huang S, Zhao X et al. Modularly assembled designer TAL effector nucleases for targeted gene knockout and gene replacement in eukaryotes. Nucleic Acids Res 2011;39:6315–6325.
60 Li T, Huang S, Jiang WZ et al. TAL nucleases (TALNs): Hybrid proteins composed of TAL effectors and FokI DNA-cleavage domain. Nucleic Acids Res 2011;39:359–372.
61 Cade L, Reyon D, Hwang WY et al. Highly efficient generation of heritable zebrafish gene mutations using homo- and heterodimeric TALENs. Nucleic Acids Res 2012;40: 8001–8010.
62 Sander JD, Cade L, Khayter C et al. Targeted gene disruption in somatic zebrafish cells using engineered TALENs. Nat Biotechnol 2011;29:697–698.
63 Tong C, Huang G, Ashton C et al. Rapid and cost-effective gene targeting in rat embryonic stem cells by TALENs. J Genet Genomics 2012;39:275–280.
64 Mussolino C, Morbitzer R, Lutge F et al. A novel TALE nuclease scaffold enables high genome editing activity in combination with low toxicity. Nucleic Acids Res 2011;39:9283–9293.
65 Hockemeyer D, Wang H, Kiani S et al. Genetic engineering of human pluripotent cells using TALE nucleases. Nat Biotechnol 2011;29:731–734.
66 Miller JC, Tan S, Qiao G et al. A TALE nuclease architecture for efficient genome editing. Nat Biotechnol 2011;29:143–148.
67 Yusa K, Rashid ST, Strick-Marchand H et al. Targeted gene correction of alpha1-antitrypsin deficiency in induced pluripotent stem cells. Nature 2011;478:391–394.
68 Sebastiano V, Maeder ML, Angstman JF et al. In situ genetic correction of the sickle cell anemia mutation in human induced pluripotent stem cells using engineered zinc finger nucleases. Stem Cells 2011;29:1717–1726.
69 Zou J, Mali P, Huang X et al. Site-specific gene correction of a point mutation in human iPS cells derived from an adult patient with sickle cell disease. Blood 2011; 118:4599–4608.
70 Urnov FD, Miller JC, Lee YL et al. Highly efficient endogenous human gene correction using designed zinc-finger nucleases. Nature 2005;435:646–651.
71 Roth DB, Wilson JH. Relative rates of homologous and nonhomologous recombination in transfected DNA. Proc Natl Acad Sci USA 1985;82:3355–3359.
72 Wansink DG, van Herpen RE, Coerwinkel-Driessen MM et al. Alternative splicing controls myotonic dystrophy protein kinase structure, enzymatic activity, and subcellular localization. Mol Cell Biol 2003;23: 5489–5501.
73 Zu T, Gibbens B, Doty NS et al. Non-ATG-initiated translation directed by microsatellite expansions. Proc Natl Acad Sci USA 2011;108:260–265.
74 Ash PE, Bieniek KF, Gendron TF et al. Unconventional translation of C9ORF72 GGGGCC expansion generates insoluble polypeptides specific to c9FTD/ALS. Neuron 2013; 77:639–646.
75 Cleary JD, Ranum LP. Repeat-associated non-ATG (RAN) translation in neurological disease. Hum Mol Genet 2013;22:R45–R51.
76 Groh M, Silva LM, Gromak N. Mechanisms of transcriptional dysregulation in repeat expansion disorders. Biochem Soc Trans 2014;42:1123–1128.
77 Budworth H, McMurray CT. Bidirectional transcription of trinucleotide repeats: Roles for excision repair. DNA Repair (Amst) 2013; 12:672–684.
78 Cho DH, Thienes CP, Mahoney SE et al. Antisense transcription and heterochromatin at the DM1 CTG repeats are constrained by CTCF. Mol Cell 2005;20:483–489.


See www.StemCells.com for supporting information available online.